

Predicting the pressure-volume curve of an elastic microsphere composite

Riccardo De Pascalis, I. David Abrahams, William J. Parnell

*School of Mathematics, University of Manchester,
Manchester M13 9PL, United Kingdom*

ABSTRACT

The effective macroscopic response of nonlinear elastomeric inhomogeneous materials is of great interest in many applications including nonlinear composite materials and soft biological tissues. The interest of the present work is associated with a *microsphere composite material*, which is modelled as a matrix-inclusion composite. The matrix phase is a homogeneous isotropic nonlinear rubber-like material and the inclusion phase is more complex, consisting of a distribution of sizes of stiff thin spherical shells filled with gas. Experimentally, such materials have been shown to undergo complex deformation under cyclic loading. Here, we consider microspheres embedded in an unbounded host material and assume that a hydrostatic pressure is applied in the ‘far-field’. Taking into account a variety of effects including buckling of the spherical shells, large deformation of the host phase and evolving microstructure, we derive a model predicting the *pressure-relative volume change* load curves. Nonlinear constitutive behaviour of the matrix medium is accounted for by employing neo-Hookean and Mooney-Rivlin incompressible models. Moreover a nearly-incompressible solution is derived via asymptotic analysis for a spherical cavity embedded in an unbounded isotropic homogeneous hyperelastic medium loaded hydrostatically. The load-curve predictions reveal a strong dependence on the microstructure of the composite, including distribution of microspheres, the stiffness of the shells, and on the initial volume fraction of the inclusions, whereas there is only a modest dependence on the characteristic properties of the nonlinear elastic model used for the rubber host.

KEYWORDS: microsphere, composite, pressure-volume curve, buckling, nonlinear elasticity, rubber, Mooney-Rivlin

1. Introduction

Microsphere composites are used in a multitude of industrial applications. Good examples are ultra-low density fillers in engineering materials such as composites, coatings, sealants, explosives, automotive components, paint and crack fillers and elastomers and as blowing agents in printing inks (Ash and Ash, 2007). The microsphere is a spherical particle, a few microns in diameter, with a thermoplastic shell, and shell to diameter ratio typically of the order of 0.01. The use of microspheres in materials brings forth numerous benefits which include reducing density, improving stability, increasing impact strength, providing a smoother surface finish, increasing thermal insulation, increasing compressibility and often reducing costs. A scanning electron microscopy image of the microstructure of a hollow glass microsphere composite (with very high volume fraction) is shown in Fig. 1 taken from Li et al. (2011).

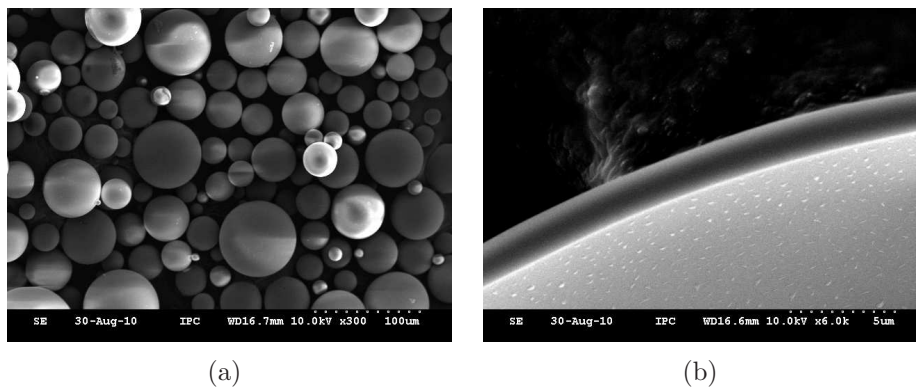


Figure 1: Scanning electron microscopy image of (a) a Hollow Glass Microsphere composite material and (b) its surface/shell structure. In this situation (with applications to thermal conductivity) the composite is densely filled with microspheres. Reproduced (with kind permission) from Li et al. (2011).

The application of interest in this paper is that of acoustics, using microsphere composites as a means of reducing sound reflection. The composite consists of an elastomeric matrix phase, inside which are located a large number of randomly distributed Expancel microspheres, see Fig. 2(a) Shorter et al. (2008). Of specific interest is how sound reflection can be affected by a macroscopic hydrostatic pressure applied to the microsphere composite. These materials have been found to be useful in such conditions

because the presence of the reinforcing shell delays the onset of the cavity collapse and the consequent degradation in the acoustic performance of the composite. In order to understand exactly how the acoustic characteristics of the material are affected by applied pressure, it is necessary to develop models that describe how the composite deforms mechanically under this applied loading. Experimentally it is known that the constitutive *pressure-relative volume change* curve is nonlinear (and hysteretic during unloading) but the dominant physical mechanisms contributing to this nonlinearity are still not fully understood. In Fig. 2(b) we illustrate the constitutive behaviour of the material with some experimentally determined load curves associated with the composite for increasing volume fractions of the microsphere material Shorter et al. (2008).

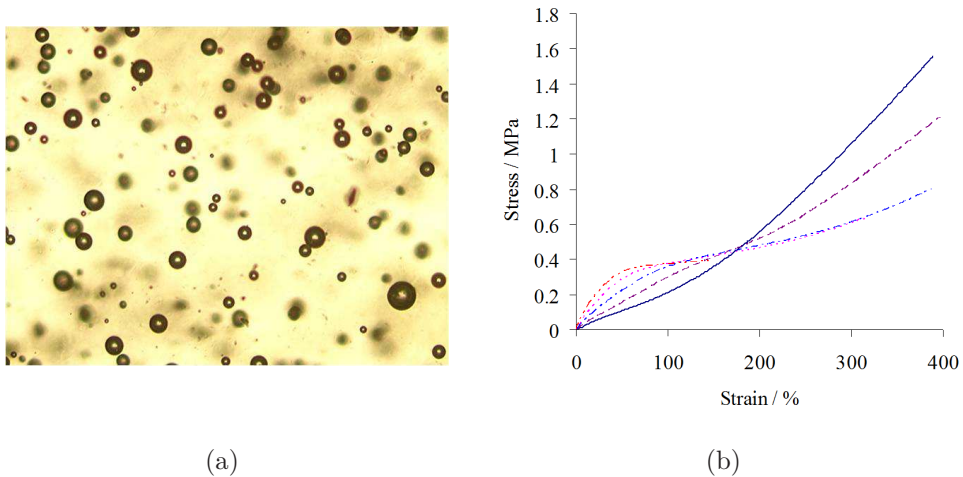


Figure 2: In (a) we show an image of a Silicone Room Temperature Vulcanizing (RTV) microsphere elastomer filled with 5% volume of Expancel microspheres. In (b) we show an experimentally determined stress-strain curve associated with this composite under uniaxial tension. The solid curve is unfilled and others refer to increasing volume fractions of the microsphere phase. Reproduced (with kind permission) from Shorter et al. (2008).

A wide range of work on the modelling of microsphere filled composites has appeared in the literature. For the prediction of their acoustic properties *without applied pressure*, a number of models have been proposed, see e.g. Gaunard and Uberall (1982) and Baird et al. (1999) in the elastic and viscoelastic case respectively. Such predictions typically rely upon the use of classical multiple scattering models, the most commonly used being those

of Waterman and Truell (1961); Kuster and Toksöz (1974); Bose and Mal (1974); Gaunaurd and Uberall (1982); Anson and Chivers (1989). We note that a useful comparison of experiments and various theories can be found in Anson and Chivers (1993).

Gaunaurd et al. (1984) considered the pressure dependence of dynamic moduli, albeit in a simplified case of porous solids, i.e. in the absence of the shell phase and thus the effect of the pressure is to reduce the pore size, the main interest lying in the dynamic material properties. Here, although we are certainly interested in the dynamic response, we wish first to understand the origins of nonlinearity in the *pressure-relative volume change* loading curve associated with the composite. Significant work has been carried out on the deformation of porous materials, see e.g. Mackenzie (1950) for an early model for associated effective linear elastic properties, and for rubber foam materials, see e.g. Gent and Thomas (1959), Gibson and Ashby (1982) and Lakes et al. (1993), where the principal mechanisms of deformation are well understood. However, the composite under consideration here has a more complex microstructure due principally to the presence of microspheres and the lack of understanding as to how they behave within the elastomeric substrate under applied pressure. Microspheres are also present in the context of syntactic foams (a material comprising a polymeric matrix filled with microspheres). Such materials open up the possibility of low density materials with high tolerance to damage. Much of the recent modelling work in this area however has focused on the effective *linear* elastic properties of the composite. A variety of static homogenization techniques have been used, see e.g. Bardella and Genna (2001); Gupta and Woldesenbet (2004); Porfiri and Gupta (2009); Tagliavia et al. (2009).

Few models deal with the nonlinear response of a microsphere composite under loading. Kerr and Baird (2002) proposed an elasto-plastic model for the load curve and subsequent prediction of dynamic material properties. One criticism of this model would be that plasticity yields permanent deformation. However, it is well acknowledged that although the load-unload curve is hysteretic, when all load has been removed the material (eventually) returns to its original configuration (Brazier-Smith, 2010). Therefore it does not appear that plastic deformation is the cause of nonlinearity. In a related application Panigrahi et al. (2008) considered the acoustic response of inhomogeneous media under applied pressure, although it appears that the microstructure is rather different from that considered here. In Shorter et al. (2008), Shorter et al. (2010) the problem of the buckling of a single, isolated

spherical shell was considered (as a result of axial compression, rather than hydrostatic pressure) using Finite Element Analysis and results were subsequently compared with experiments involving a table tennis ball embedded inside a transparent elastomer. Comparisons were made between perfectly bonded and unbonded spherical shells and subsequent buckling response. The principal argument of the paper was to propose that microsphere buckling is a dominant contributor to the nonlinear behaviour of the pressure-relative volume change curve.

The computational work carried out in Shorter et al. (2008) suggests that a model incorporating microsphere buckling could successfully predict the nonlinearity of the load curve. Therefore here we develop a fundamental mathematical model for the loading portion of the pressure-relative volume change curve by incorporating volumetric changes and local microsphere shell buckling effects. We assume that there is a distribution of shell to radius ratio thicknesses and we will suppose that the microspheres are distributed dilutely, so that interaction effects between microspheres can be neglected. Interaction effects will be considered in future work.

In order to incorporate the effect of buckling of the microsphere shell, we must understand how a spherical shell buckles inside an elastic medium under far-field hydrostatic pressure. Although a great deal of classical work exists regarding the buckling of spherical shells (where the imposed pressure is on the surface of the shell itself), see for example Wesolowski (1967); Koiter (1969); Wang and Ertepinar (1972) and more recently Fu (1998); Ben Amar and Goriely (2005), there is a surprising lack of work regarding the buckling of shells (of any geometry) that are embedded inside another medium. Of specific interest is how the host medium affects the classical buckling pressure.

Initial work into the buckling pressure of a spherical shell embedded in an unbounded uniform elastic medium has been carried out by Fok and Allwright (2001) and Jones et al. (2008). We shall discuss these models and their assumptions later on in the paper, particularly that of Fok and Allwright (2001) which is the model that we shall adopt for buckling here. As described above, Shorter et al. (2008) also carried out some experimental work related to this problem.

The fundamental objective here then is to determine a model for the loading portion of the *pressure-relative volume change curve* by considering a distribution of shell thickness to radius ratio of microspheres which are dilutely dispersed throughout the material. We also introduce nonlinear (finite)

elasticity in order to incorporate large deformation of the rubber composite in the post-buckling regime. The theory provides a modelling tool to assess certain likelihood scenarios. In particular we are able to assess the sensitivity of effective properties to changes in specific parameters, e.g. distribution of microspheres, nonlinearity and constitutive behaviour of the constituent materials that make up the composite and the gas law inside microspheres.

2. Preliminaries and background

We consider a composite material with two constituents (or *phases* as we shall term them here) known as the matrix and inclusion phase. The matrix phase is a (possibly compressible) homogeneous rubber material and the inclusion phase consists of a distribution of thin spherical shells (possibly filled with some gas) of initial radius A and shell thickness H . We allow for the possibility of a distribution of microsphere shell thickness to radius ratios $X = H/A$. This distribution is governed by a probability distribution function $F(X)$. The volume fraction of the inclusion phase is denoted by Φ . We are specifically interested in the problem where the material is subjected to an external hydrostatic pressure \hat{p} . We shall state all pressures relative to atmospheric pressure p_{ATM} so that upon defining $p = \hat{p} - p_{\text{ATM}}$, $p = 0$ corresponds physically to atmospheric pressure. Similarly, we assume that the gas inside the microspheres is also initially at atmospheric pressure so that denoting \hat{p}_{IN} as the internal hydrostatic pressure we can initially set $p_{\text{IN}} = \hat{p}_{\text{IN}} - p_{\text{ATM}} = 0$. Henceforth all pressures are thus defined relative to atmospheric pressure.

Consider for the moment a single microsphere embedded in an *unbounded* matrix material so that we assume that the pressure is applied in the ‘far-field’. At a critical far-field pressure p_c , this shell will buckle and the microsphere will lose its compressive rigidity for $p > p_c$. Since we assume that we have a distribution of microspheres, each with a different $X = H/A$, the microspheres will buckle successively as the external pressure is continuously increased. We illustrate this in Fig. 3. The prediction of the pressure-volume relation, given the volume fraction Φ of microspheres, the constitutive behaviour of the matrix phase, the elastic properties of the microsphere shell, the knowledge of gas internal to the microspheres and the overall distribution of X , is clearly a non-trivial problem. The effects of interaction on buckling have thus far not been studied and therefore here we consider the case where buckling of a microsphere depends only on the far-field hydrostatic pressure p

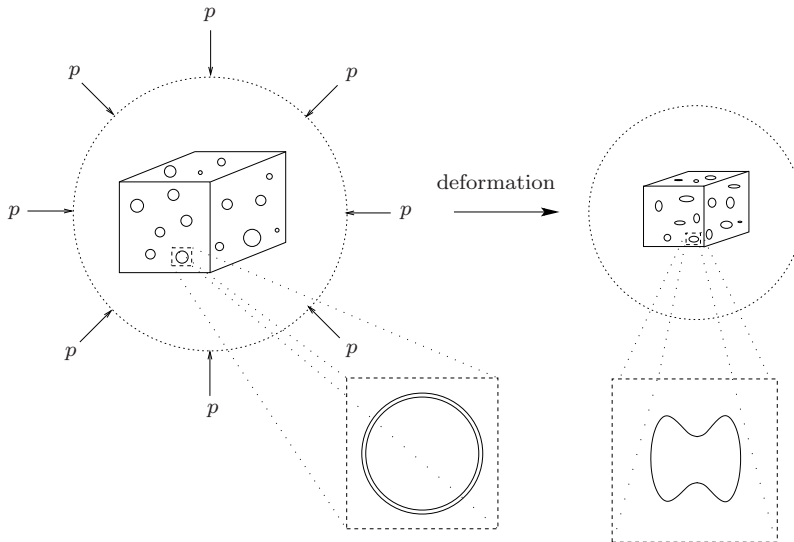


Figure 3: A cube of the microsphere composite material (no scale is implied) is subjected to hydrostatic pressure p in the far field with inset figure indicating that the microspheres are spherical pre-buckling. This spherical symmetry is retained until the onset of buckling, after which the shells deform significantly, losing their rigidity in this state, as indicated in the figure inset. We do not indicate the precise structure of the shell post-buckling: this requires detailed post-buckling analysis.

and *not* on the influence of other microspheres. We anticipate therefore that this model is valid for a dilute dispersion of microspheres. We note however, that in many homogenization theories, it is often surprising how accurate dilute dispersion theories are even in the non-dilute regime (Parnell et al., 2010). Later work will consider interaction effects in more detail.

We shall consider each microsphere to have a fixed initial radius A and let the shell thickness H vary, so that $X = H/A$ is governed by a probability distribution function $F(X)$. Alternatively we could consider H fixed and vary A but it transpires that the analysis of the former is more straightforward. (Note that for a single microsphere inclusion the scale invariance means that varying A or H for any fixed X must yield the same result.) In some cases we need to refer to the middle surface of the shell whose radius we denote by $\hat{A} = A - H/2$, and the shell thickness to middle radius ratio as $\hat{X} = H/\hat{A}$. Also the probability distribution function can therefore be given in terms of \hat{X} , i.e. $F(\hat{X})$. With reference to Fig. 4 we define a (fictitious) radius $S > A$ by the condition $\Phi = (A/S)^3$ where Φ is the prescribed volume

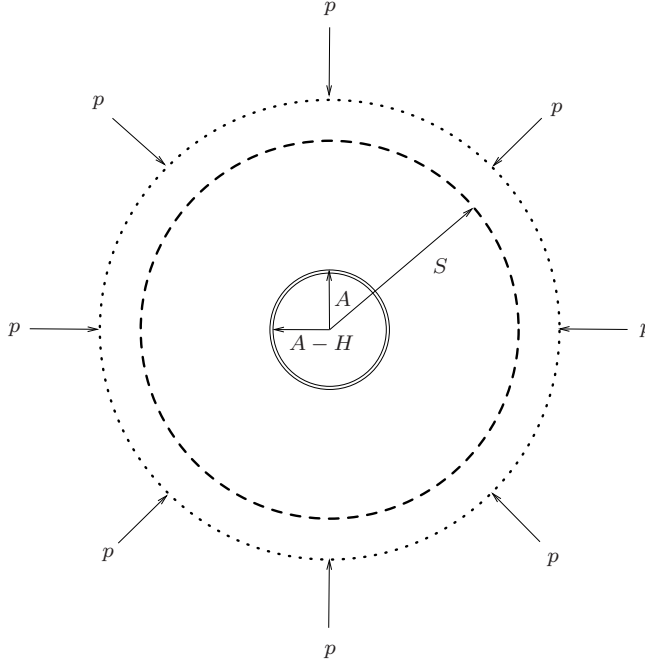


Figure 4: A single ‘composite sphere’ loaded by the hydrostatic far-field pressure p .

fraction of microspheres. We then consider how the material deforms, and how the microsphere buckles, given some hydrostatic pressure p in the far-field with this region inside S (containing the microsphere and which we will term the *composite sphere* (CS)) embedded in a purely matrix material. The prescription of the radius S allows us to consider the volume change of the matrix region under compression.

We denote by κ, μ, E, ν the bulk, shear and Young’s moduli and Poisson’s ratio respectively from linear elasticity and we note the relations $\nu = (3\kappa - 2\mu)/(2(3\kappa + \mu))$ and $E = 9\kappa\mu/(3\kappa + \mu)$ since later we usually specify μ and κ . We will make use of the subscripts s and m when we wish to refer to the shell and to the matrix medium, respectively.

Before the microsphere shell buckles (which we shall term the *pre-buckling* stage) we consider the elastic behaviour of both the matrix and microsphere shell to be linear. As will be shown, this is reasonable since the shell stiffness is significantly higher than that of the matrix phase and therefore induced strains in both media will be small (see also section 7 in Jones et al. (2008) for more details). After the microsphere shell buckles (which we term the

post-buckling stage) we make the assumption that the shell will lose almost all of its rigidity and therefore that the post-buckled microsphere can be replaced by a cavity (whilst still ensuring continuity of displacement and traction between the matrix and fluid as we shall show later). In this post-buckling regime we incorporate nonlinear elastic behaviour by permitting large strains and also nonlinear constitutive behaviour.

In order to justify the linear pre-buckling and nonlinear post-buckling assumptions, respectively, we consider the following example. We are here interested in understanding how the stiffness of the shell can make the material more rigid as compared with the case when the shell is absent. To this end we can consider for example the case of a thin glassy shell (see Baird et al. (1999)), with surrounding polymeric elastomer composed of a polyurethane material. The matrix Young's modulus can be taken as $E_m = 3.6$ MPa and Poisson ratio is typically close to 0.5 (Diaconu and Dorohoia, 2005). In terms of bulk and shear moduli, we choose the parameter set

$$\begin{aligned} \mu_s &= 1.26 \text{ GPa}, & \kappa_s &= 2.1 \text{ GPa}, \\ \mu_m &= 1.2 \text{ MPa}, & \kappa_m &= 4 \text{ GPa}. \end{aligned} \tag{1}$$

Note that with this choice, $\nu_m = 0.49985$ i.e. the matrix is considered essentially incompressible. Next, let us take a microsphere with shell to radius ratio $X = 0.01$ and for an imposed scaled far-field pressure p/μ_m , we evaluate the scaled displacement (with notation reported in section 3.1) $u_r^m(A)/A$ at $r = A$ (the radius at which the displacement is maximum). In Fig. 5 we plot this maximum displacement as a function of the imposed pressure when the shell is and is not present (left and right on the figure, respectively) and in both cases we note that this is predicted by linear elasticity theory. The dashed line denotes the critical pressure for this shell to radius ratio, predicted by the Fok-Allwright buckling criterion (8) (Fok and Allwright, 2001). When the shell *is* included, values of $u(A)_r^m/A$ remain small for applied pressures below this critical value (see the left side of Fig. 5). On the contrary, in the absence of the shell, when reasonable values of the pressure are applied, the linear theory is no longer appropriate due to the large values of the scaled displacements $u_r^m(A)/A$ in this case (see the right side of Fig. 5). We conclude that in this latter regime we *must* therefore incorporate full nonlinearity in order to permit finite deformations.

Although we are concerned with matrix materials that ostensibly behave incompressibly (typically μ_m/κ_m is small, in particular of the order of 10^{-4} ,

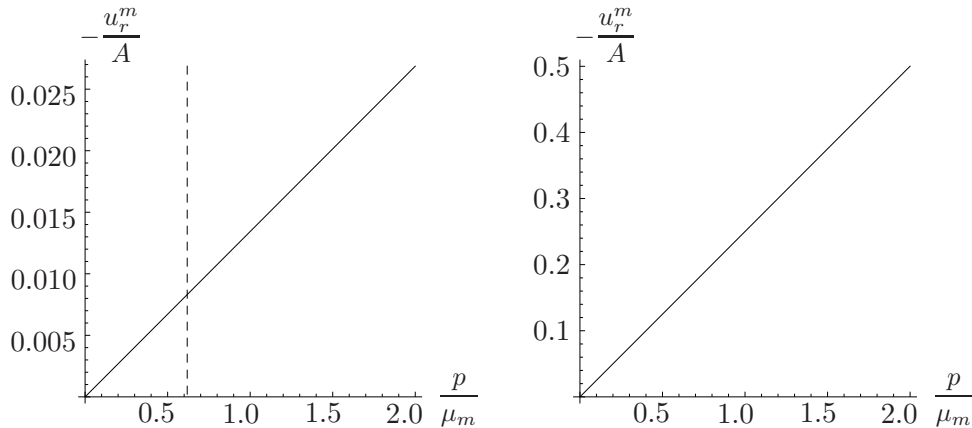


Figure 5: Plot of the the scaled radial displacement $u(A)_r^m/A$ determined using linear elasticity when the shell is (left) and is not (right) included in the model. Associated values of X used are $X = 0.01$ and $X = 0$ respectively. The dashed line is the critical pressure predicted by (8).

see Ogden (1976)), in section 4.2 we also calculate the volume change post-buckling for a *nearly-incompressible* theory. As will be shown, it is difficult to distinguish the difference between results for the slightly-compressible and incompressible cases, as should be expected.

3. Pre-buckling behaviour and the buckling model

In the pre-buckling stage, we consider both shell and matrix phase to be compressible linear elastic materials (noting that the matrix is almost incompressible) which are perfectly bonded, and we assume that gas resides inside the microsphere providing a constant internal pressure p_{IN} . We wish to determine the total volume change (relative to the initial volume) of the material and in order to do this we determine the volume change in the composite sphere (CS) when the pressure p is imposed at infinity.

3.1. Linear elasticity

Under the assumption of linear isotropic elasticity, the governing equations of the corresponding static boundary value problem with no body forces are given as follows

$$\sigma_{ij,i} = 0, \tag{2}$$

$$\epsilon_{ij} = \frac{1}{2}(u_{i,j} + u_{j,i}), \quad (3)$$

$$\sigma_{ij} = \lambda\epsilon_{kk}\delta_{ij} + 2\mu\epsilon_{ij}, \quad (4)$$

where σ_{ij} , ϵ_{ij} , and u_i are the components of the stress and strain tensors, and the displacements, respectively and we have introduced the Kronecker delta tensor δ_{ij} . The matrix material is homogeneous with Lamé constants λ, μ where $\lambda = \kappa - 2\mu/3$. Since the problem is linearly elastic, geometry is spherically symmetric and a purely radial stress is applied, then spherical symmetry is preserved ($u_r = u_r(r), u_\theta = u_\phi = 0$). Hence, equation (2) reduces to a single second order ordinary differential equation which is independent of the Lamé moduli. The general solution for the displacement in the shell and medium region is therefore of the form

$$u_r^i(r) = A_i r + \frac{B_i}{r^2}, \quad (5)$$

where $i = s, m$ refers to the shell and matrix respectively, and A_i, B_i are constants that are fully determined by imposing continuity of displacement and radial stress on $r = A$ and the following loading boundary conditions

$$\sigma_{rr}^s(A - H) = -p_{\text{IN}}, \quad \sigma_{rr}^m(r) \Big|_{r \rightarrow \infty} = -p. \quad (6)$$

3.2. Pre-buckling: relative volume change for each CS

Let us consider a single CS of initial radius S and volume V containing a microsphere of undeformed radius A and $X = H/A$. When we increase the far-field pressure p ($0 < p < p_c$), this volume $V = (4/3)\pi S^3$ reduces to $v = (4/3)\pi s^3$, where $s = S + u_r^m(S)$ denotes the deformed radius of the CS, referring to (5). The relative volume change, say δv , occurring in the pre-buckling stage is therefore given by

$$\delta v = \frac{V - v}{V} = 1 - \left(\frac{s}{S}\right)^3. \quad (7)$$

Note that we have assumed the inner pressure inside the microsphere to remain constant under loading. This appears to be reasonable since volume changes will be small, but will not remain valid in the post-buckling regime as we shall consider in section 4.

3.3. Microsphere buckling

In this section we discuss the buckling of a spherical shell inside an unbounded elastic matrix medium, loaded by a far-field hydrostatic pressure p . We employ a buckling model introduced by Fok and Allwright (2001). Given a distribution of sizes of microspheres inside the material, our aim is to determine which of them, for a given imposed pressure p , have buckled and which remain unbuckled.

In Fok and Allwright (2001) a criterion was derived for the buckling of a spherical shell embedded in an elastic material and loaded by a far-field hydrostatic pressure under the main assumptions that deformations are axisymmetric and the shell is inextensible. They also neglected the inner gas pressure, so in our model we must set $p_{\text{IN}} = 0$ in the pre-buckling phase. This latter simplification is, in fact, not too severe as the displacement is affected very little by internal pressure pre-buckling. The assumption of axisymmetric buckling is not a restriction; Wesolowski (1967) showed that the critical mode number for buckling is the same whether the eigenmode is symmetric or not. Also, for glassy shells in the present model, it is easy to show that the assumption of inextensibility is consistent with the estimates found for the radial and shear stresses.

Fok and Allwright (2001) obtained a formula for the critical pressure $p(\hat{X}, n)$ in the form

$$\frac{p(\hat{X}, n)}{E_s} = \frac{2}{3} \frac{1 + \nu_m}{1 - \nu_m} \left(1 + \frac{1 - \nu_s}{1 + \nu_m} \frac{E_m}{E_s} \frac{1}{\hat{X}} \right) \left(p_1(n) \hat{X}^3 + p_2(n) \hat{X} + p_3(n) \right) \quad (8)$$

where $\hat{X} = H/\hat{A}$ and n are the shell thickness to *middle* radius ratio of the microsphere and the mode number respectively. Note that in the Fok-Allwright approach, n is a natural number greater than 1; dilatational ($n=0$) and rigid-body ($n=1$) modes are not considered. The functions p_1, p_2 and p_3 are given by

$$\begin{aligned} p_1 &= [n(n+1) - (1 - \nu_s)] / 12(1 - \nu_s^2), & p_2 &= 2 / [(n-1)(n+2)(1 + \nu_s)] \\ p_3 &= E_m / E_s \frac{(2n^3 - n^2 + 3n + 2) - \nu_m(2n^3 - 3n^2 + 5n + 2)}{(n-1)^2(n+2)(3n+2 - 2\nu_m(2n+1))(1 + \nu_m)}. \end{aligned} \quad (9)$$

The standard approach would be to specify the shell ratio \hat{X} and material constants ν_s, ν_m, E_s, E_m and substitute these into (8) to give the critical buckling pressure found by minimizing with respect to n (and thus this also gives

the corresponding buckling mode n). Here, however we need to approach the problem slightly differently since we have a distribution of microsphere sizes and we wish to know what the state of that distribution of microspheres (buckled/unbuckled) is at a given pressure. It will prove convenient, therefore, to treat n as a parameter as we now explain. Assuming \hat{X} is for now *unspecified*, by a continuity argument, assuming that $n > 1$ is a given real number we determine the minimum by insisting that $\partial p(\hat{X}, n)/\partial n = 0$ and solve for \hat{X} . From trivial algebraic considerations it is straightforward to show the existence of a minimum for $p(\hat{X}, n)$ via

$$p'_1(n)\hat{X}^3 + p'_2(n)\hat{X} + p'_3(n) = 0 \quad (10)$$

where prime denotes differentiation with respect to argument. The real positive root \hat{X} in (10) depends on the mode number n , which we denote by $\hat{X}_c(n)$ where the subscript c refers to *critical*. Thus, we specify $n \in (1, \infty)$, determine the corresponding \hat{X}_c from (10), and then the corresponding $p_c = p(\hat{X}_c, n)$ from (8). In this manner we therefore know that shells in the range $\hat{X} \leq \hat{X}_c$ are buckled whereas those for $\hat{X} > \hat{X}_c$ remain unbuckled.

In Fig. 6 we plot the predictions given by the Fok and Allwright (2001) model for the critical pressure p_c as a function of critical size \hat{X}_c , letting the buckling mode parameter n lie in the range $[13, 1000]$, assuming $p_{\text{IN}} = 0$ and given the material constants in (1). This range of buckling modes gives rise to realistic pressures; choosing a lower n corresponds to a higher pressure.

4. Post-buckling behaviour: nonlinear elastic response

As we have emphasized before, as we increase the hydrostatic load p gradually, an increasing number of shells will transition to a buckled state. When the shell buckles, there will be some complex modification to the structure of the shell and the local matrix medium. Buckling of the shell will result in a local loss of rigidity and (initially at least) a macroscopic increase in compressibility. Modelling the exact modification to the numerous shell structures is a formidable task and hence from a modelling viewpoint, in order to model the post-buckling behaviour we shall make the following simplification. For pressures $p > p_c$, for a CS region, we assume that the spherical shell region is replaced by a spherical cavity, which at the pressure p_c , has the same radius as the microsphere at its buckling pressure. The post-buckling stage of behaviour will be analyzed under the nonlinear deformation

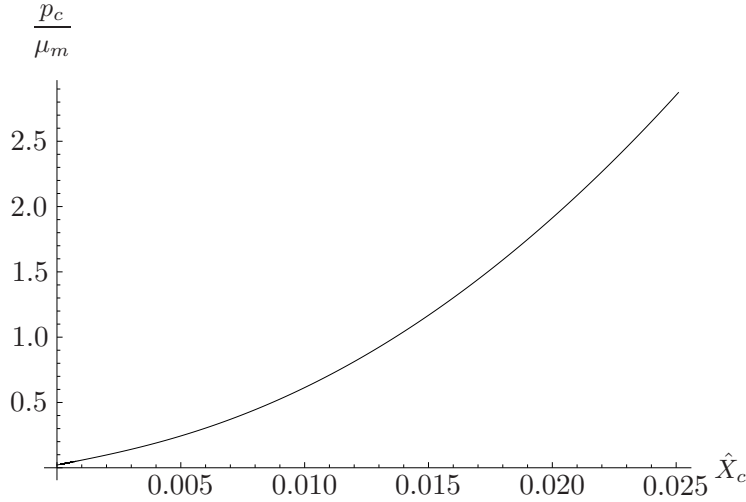


Figure 6: Plot of the critical hydrostatic pressure p_c/μ_m as a function of the critical ratio \hat{X}_c predicted by the Fok and Allwright (2001) model, obtained for $n \in [13, 1000]$, when we use the material constants specified in (1) and we assume $p_{\text{IN}} = 0$.

assumption, because the loss of rigidity of the microsphere will permit finite deformations if appreciable pressure p/μ_m is applied (note again Fig. 5). We wish to understand how an additional increase in pressure in the CS region, past the buckling pressure p_c , decreases the volume of the CS further and subsequently we shall derive this influence on the macroscopic volume of the composite material.

From the pre-buckling analysis we can determine exactly the predictions of the deformed radii s_c and a_c of the CS (with corresponding initial radii S and A respectively) where the subscript c indicates the critical value at the buckling pressure p_c . We can therefore begin our nonlinear analysis from those values, further increasing the load pressure until we reach the chosen load p . This two stage linear-nonlinear approach is however not particularly appealing; in fact we are able to consider the volume change in the post-buckling regime by considering an alternative (nonlinear) problem from the outset (i.e. increasing the far-field pressure from zero) that is statically equivalent to the linear problem in the pre-buckling regime as we shall now show.

With reference to Fig. 7, consider a full nonlinear elasticity formulation of the deformation associated with an unstressed medium within which resides a *cavity* with the same radius A as the initially undeformed microsphere. We consider the deformation of the spherical cavity due to a far-field pressure with an additional internal ‘shell pressure’ denoted by p_{IN}^s which mimics the

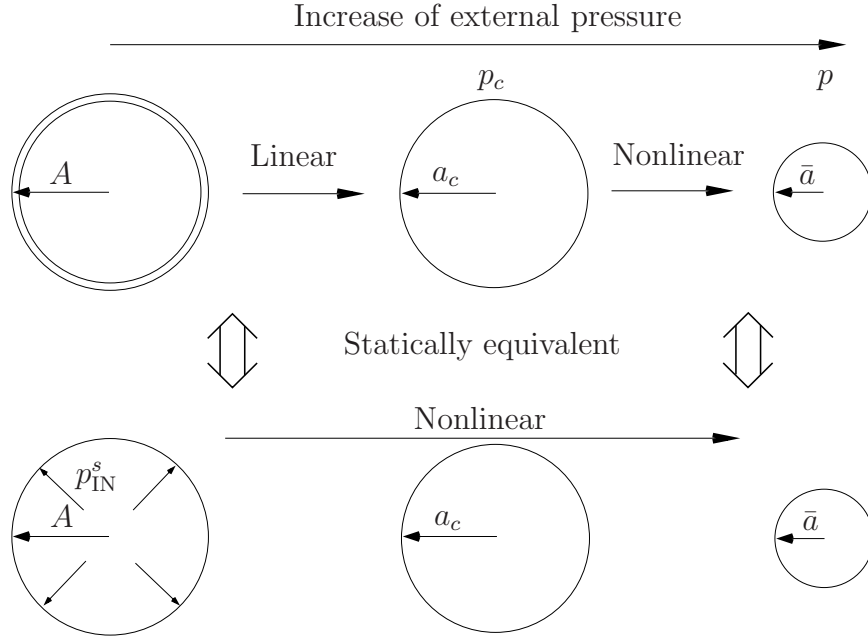


Figure 7: To determine the nonlinear deformation post-buckling we use a problem that is statically equivalent to the true problem which is drawn schematically here. Above is the linear-nonlinear process of deformation and below the fully nonlinear process. The presence of the shell is represented by the internal pressure p_{IN}^s in the latter, which ensures the correct radius when $p = p_c$.

residual presence of the shell. We choose this pressure by referring to the (linear) pre-buckling analysis, considering this to be the maximum pressure that the shell exerts on the matrix pre-buckling, i.e.

$$p_{\text{IN}}^s = -\sigma_{rr}^m(A), \text{ at } p = p_c, \quad (11)$$

such that at the critical pressure we recover to a good approximation the linear elastic solution, i.e. to obtain agreement for a_c and s_c . This therefore gives the correct starting point for volume change calculations for $p > p_c$.

We shall consider several assumptions for the nonlinear elastic matrix, and we make use of a *bar* on quantities in the post-buckling regime, in particular the undeformed radii A, S and the initial volume V are now denoted by \bar{a} , \bar{s} , and \bar{v} respectively.

We must now determine the deformation of the cavity subject to the imposed external pressure. Since this is spherically symmetric we assume that

the deformation is purely radial and we therefore write this *radial deformation* in spherical polar coordinates as

$$r = r(R), \quad \theta = \Theta, \quad \phi = \Phi, \quad (12)$$

where (R, Θ, Φ) are the polar coordinates in the reference configuration and (r, θ, ϕ) are the polar coordinates in the current configuration, respectively, with $dr/dR > 0$. From the result of Ericksen (Ericksen, 1955) this deformation is not a controllable deformation that is possible in every *compressible* homogeneous and isotropic hyperelastic material. Therefore this *inhomogeneous* deformation for compressible materials has to be discussed in the context of special materials. For example for a special *Blatz-Ko material* an analytical solution has been found in a parametric way (Chung et al., 1986; Horgan, 1989, 1995). Six other classes of compressible materials have received much attention in the literature where the solution can also be found analytically (Carroll, 1988, 1991a,b; Murphy, 1992). For an overview of such results see Horgan (2001).

In the incompressible case, thanks to the constraint of incompressibility, the radial deformation (12) can be treated in a much more straightforward manner and indeed is a universal solution (we refer to section 57 of Truesdell and Noll (1992) for more details). This deformation satisfies the balance equations with zero body force, its equilibrium is supported by suitable surface tractions alone, and is the same for all materials (in the class of *constrained* materials). The choice of strain energy function therefore merely dictates the stress field induced by the deformation.

The special compressible solutions for radial deformation referred to above are not well suited to describe the constitutive response of a rubber-like material and therefore we choose not to use these here. Our analysis is therefore concerned firstly with purely incompressible materials before we move on to describe nearly-incompressible materials in the context of an asymptotic theory with a small parameter $\mu/\kappa \ll 1$. In the latter case we use a constitutive model proposed in the literature by Horgan and Murphy (2009) which was based on experimental behaviour (see for example Penn (1970)).

For ease of exposition we have placed details of the theory of nonlinear elasticity associated with the subsections to follow in Appendix A.

4.1. Post-buckling with incompressibility

The polar components of the deformation gradient associated with (12) are given by

$$\mathbf{F} = \text{diag}(dr/dR, r/R, r/R) \quad (13)$$

and for an incompressible material the constraint of incompressibility $\det \mathbf{F} = 1$ states that

$$r(R) = (R^3 + \alpha)^{1/3}, \quad (14)$$

where $\alpha = \bar{a}^3 - A^3$. The equilibrium equations in the absence of body forces are $\text{div} \mathbf{T} = 0$ where \mathbf{T} is the Cauchy stress tensor. In the radially symmetric case these reduce to the single ordinary differential equation

$$\frac{dT_{rr}}{dr} + \frac{2}{r} (T_{rr} - T_{\theta\theta}) = 0 \quad (15)$$

where \mathbf{T} is derived from a *strain energy function* (SEF) W , as described in Appendix A. In this subsection we shall consider two incompressible models, the neo-Hookean material with SEF W_{NH} and Mooney-Rivlin material with SEF W_{MR} , whose forms are given in Appendix A.

Up to the point of buckling note that we have assumed that the pressure inside the microsphere p_{IN} is zero since changes in volume were very small. In the post-buckling stage we require the additional pressure p_{IN}^s initially to maintain continuity as described in Fig. 7 but we shall also now assume that the inner pressure p_{IN} can be non-constant. This is motivated by the fact that volume changes can now be large and therefore in this post-buckling stage at some point the gas interior to the cavity can be compressed so much as to act to stiffen the material. We therefore may anticipate a Boyle's law type relation for a massless ideal gas, of the form

$$p_{\text{IN}} = p_{\text{IN}}^s + p_{\text{IN}}^b \quad (16)$$

where p_{IN}^s is a constant that accounts for the residual effect of the buckled shell and

$$p_{\text{IN}}^b = p_{\text{ATM}} \left(\left(\frac{A}{\bar{a}} \right)^{3\eta} - 1 \right). \quad (17)$$

In the latter expression the pressure and volume are related through a polytropic exponent relationship, for a diatomic gas, with exponent $\eta = 1.4$ where η is the heat capacity ratio. Note that all pressures are stated relative to atmospheric pressure, which motivates the form in (17).

Given a SEF W , it is straightforward to integrate (15) and apply the traction boundary conditions

$$T_{rr}(R)\Big|_{R \rightarrow \infty} = -p, \quad T_{rr}(A) = -p_{\text{IN}} = -p_{\text{IN}}^s - p_{\text{IN}}^b \quad (18)$$

in order to obtain an expression linking the deformed inner radius \bar{a} and the imposed pressure difference. For the *neo-Hookean* case we obtain

$$\frac{p - p_{\text{IN}}^s - p_{\text{IN}}^b}{\mu_m} = \frac{1}{2} \left(\frac{A}{\bar{a}} \right)^4 + 2 \left(\frac{A}{\bar{a}} \right) - \frac{5}{2}, \quad (19)$$

whereas for the *Mooney-Rivlin* model, we find

$$\begin{aligned} \frac{p - p_{\text{IN}}^s - p_{\text{IN}}^b}{\mu_m} = & \left(\frac{1}{2} + \gamma \right) \left[\frac{1}{2} \left(\frac{A}{\bar{a}} \right)^4 + 2 \left(\frac{A}{\bar{a}} \right) - \frac{5}{2} \right] + \\ & \left(\frac{1}{2} - \gamma \right) \left[\left(\frac{A}{\bar{a}} \right)^2 - 2 \left(\frac{\bar{a}}{A} \right) + 1 \right]. \quad (20) \end{aligned}$$

Note that γ is a material constant with $-1/2 \leq \gamma \leq 1/2$, and when $\gamma = 1/2$ in (20), we recover the neo-Hookean solution (19).

Using the expressions (19) or (20) for \bar{a} , from (14) we can then obtain the (post-buckling) deformed radius of the CS, i.e. $\bar{s} = r(S)$, predicted by the neo-Hookean (A.3) or Mooney-Rivlin (A.4) models, respectively.

4.2. Post-buckling with slight compressibility

A great deal of work has been presented in the literature regarding the constrained theory of elasticity (e.g. incompressible materials) where many solutions have been obtained in order to describe approximations to real materials. They are approximations because of course no material is in reality completely incompressible. Numerous constitutive models have been proposed in order to model the true behaviour of the material when there is a slight deviation from incompressibility. We assume, as before, that the material is homogeneous, isotropic, and hyperelastic. The early contribution to this theory was from Spencer (1970) and an application was considered by Faulkner (1971) who considered the time dependent radial deformation of a thick walled spherical shell of almost incompressible material. More recent work has been described by Ogden (Ogden, 1976, 1978, 1997) and

Horgan and Murphy (Horgan and Murphy, 2007a,b, 2009). In order to describe the linearity between pressure and volume change (assumed to hold for pressures up to 50 MPa) summarized by Penn (1970) for natural rubber, Horgan and Murphy (2009) derived several different forms of the strain energy function and we take the form W_{HM} in (A.7).

In the case of slight compressibility, we have

$$\epsilon = \frac{\mu_m}{\kappa_m} \ll 1. \quad (21)$$

We then consider a regular perturbation problem, seeking asymptotic expansions in powers of ϵ for the relevant solutions, with the results obtained in section 4.1 arising as the leading order terms. Thus, we anticipate that the leading order deformation will be described by (14) and we seek corrections to this, associated with the strain energy function (A.7). We thus derive the deformed radii \bar{a} and \bar{s} which are slightly modified according to the slight compressibility of the matrix.

We assume that we can write for the deformed radial coordinate

$$r(R) = r_0(R) + \epsilon r_1(R) + \epsilon^2 r_2(R) + O(\epsilon^3), \quad (22)$$

where

$$r_0(R) = (R^3 + \alpha)^{1/3} \quad (23)$$

is determined from the incompressible theory (equivalently $\epsilon \rightarrow 0$).

Employing the asymptotic scheme, whose details we provide in Appendix A for ease of exposition, we derive the correction term $r_1(R)$ in (22) as that given in (A.16). This allows us to derive the additional volume change due to the compressibility of the matrix medium.

4.3. Post-buckling: relative volume change for each CS

For $p \geq p_c$, let us consider an initial composite sphere of radius S containing a microsphere of initial size $X = H/A$. The relative volume change for a buckled microsphere is now given by

$$\delta\bar{v} = \frac{V - \bar{v}}{V} = 1 - \left(\frac{\bar{s}}{S}\right)^3, \quad (24)$$

where $\bar{s} = r(S)$. For an incompressible matrix therefore \bar{s} is evaluated via (14) for Neo-Hookean or Mooney-Rivlin materials. Alternatively, for a slightly compressible matrix with strain energy function (A.7) it is evaluated via (22).

5. Predicted pressure-relative volume change curves for the microsphere material

5.1. Total relative volume change for the material

In sections 3.2 and 4.3 we calculated the relative volume change for each composite sphere associated with the pre-buckling and post-buckling stages respectively. The choice of the former or the latter depends upon whether the value of the applied pressure is below or above the theoretical critical pressure required to buckle the microsphere of shell thickness to radius ratio X in the composite sphere, according to the Fok-Allwright theory. Our principal goal is now to use these two models in order to predict the pressure-relative volume change curve for the material as a whole when there is a distribution of different shell thicknesses.

Let us introduce a probability distribution function $F(\hat{X})$ which describes the distribution of the microsphere shell thickness to radius ratios. Thus we impose the far-field hydrostatic pressure p and then use the buckling model in section 3.3 to predict the critical X_c below and above which buckling will and will not occur respectively. In this way we establish, at each given pressure p , the proportion of microspheres that are in a buckled state. Then, in order to determine the macroscopic pressure-relative volume change curve, we use (7) and (24) for that proportion of microspheres that are in the pre-buckled and post-buckled states.

The relative volume change of the entire material, say $\delta\mathcal{V}$, is therefore given by the sum of all of the relative volume changes in each composite sphere, the distribution of X being accounted for by the probability distribution function $F(\hat{X})$. As such we write

$$\delta\mathcal{V}(p) = \int_0^2 \left(\delta\bar{v}(\hat{X})\bar{\chi}(\hat{X}) + \delta v(\hat{X})\chi(\hat{X}) \right) F(\hat{X}) \, d\hat{X}. \quad (25)$$

where $\chi(\hat{X}) = 1 - \bar{\chi}(\hat{X})$ is the indicator function, defined as

$$\chi(\hat{X}) = \begin{cases} 0, & \hat{X} \in [0, \hat{X}_c], \\ 1, & \hat{X} \in [\hat{X}_c, 2]. \end{cases} \quad (26)$$

Note that in (25) we have allowed \hat{X} to take on all possible values $\hat{X} \in [0, 2]$ corresponding to $H \in [0, A]$. However, we note that the buckling theory

above is applicable to thin shells only and therefore the choice of F is important in order for (25) to give an accurate prediction. In reality the microsphere shells are very thin ($O(0.01)$) and thus the distribution function F must model this, as we now describe.

5.2. Parameter studies

Let us now consider how the *pressure-relative volume change* curve is affected by the numerous parameters in the problem and in particular we wish to understand the *sensitivity* of the curve to these parameters. We first consider the form of the probability distribution function $F(\hat{X})$. From Brazier-Smith (1999) it appears that the microsphere shell to radius ratio distribution can be described well by a Gamma distribution. We thus define

$$F(\hat{X}) = \left(\frac{k}{\hat{X}_0}\right)^k \frac{\hat{X}^{k-1}}{\Gamma(k)} \exp\left[-\left(k/\hat{X}_0\right)\hat{X}\right], \quad (27)$$

where $k > 0$ is the shape parameter, $\hat{X}_0 > 0$ is the mean value (expectation) of \hat{X} and $\Gamma(k)$ is the Gamma function evaluated at k .

Parameter studies will involve choosing values for the elastic properties $(\kappa_s, \kappa_m, \mu_s, \mu_m)$, the initial volume fraction Φ of microspheres, the parameters k and \hat{X}_0 in (27) and the constitutive model for the nonlinear elastic matrix described in section 4. Additionally we must decide whether or not to incorporate Boyle's law inside the microspheres during compression. This parameter set can therefore be chosen in many ways. We select certain cases in order to illustrate specific aspects of the model and hence test the sensitivity of the results to the particular parameters.

5.2.1. Influence of nonlinear elastic constitutive model

We start by fixing the material properties as those given in (1) and we take an initial volume fraction of microspheres as $\Phi = 0.05$. Furthermore, within the distribution function $F(\hat{X})$ given in (27) we take the shape parameter $k = 8$ as given in Brazier-Smith (1999) and we consider a mean value $\hat{X}_0 = 0.01$. Finally, we assume that the gas inside the microspheres remains at a constant atmospheric pressure, i.e. $p_{\text{IN}}^b = 0$. On the left of Fig. 8 we plot the predicted pressure-relative volume change curve for three different nonlinear elastic constitutive models in the post-buckling regime: Neo-Hookean (dotted), Mooney-Rivlin with $\gamma = 1/18$ (solid) and slightly compressible Horgan-Murphy (dashed) as well as a purely linear elastic deformation (dot-dashed).

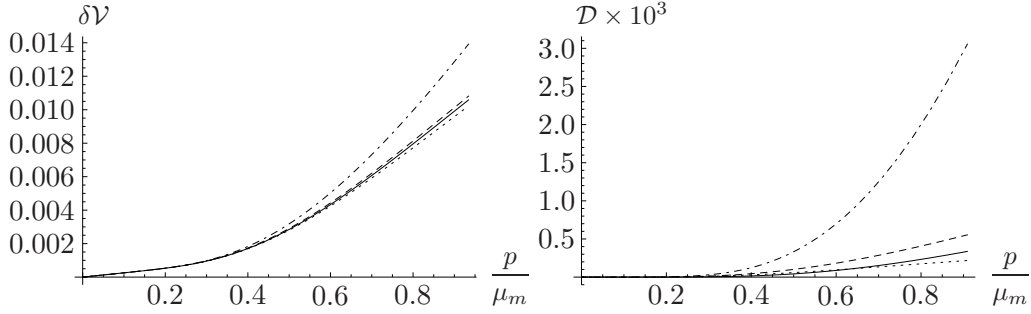


Figure 8: Left: Predicted pressure-relative volume change curve with fixed parameters $\Phi = 0.05$, $\mu_s, \kappa_s, \mu_m, \kappa_m$ as given in (1) and $F(\hat{X})$ as in (27) with $\hat{X}_0 = 0.01, k = 8$. Nonlinear model for the matrix is taken as neo-Hookean (dotted), Mooney-Rivlin (solid) and slightly-compressible Horgan Murphy (dashed) with $\gamma = 1/18$ and for reference we also plot the response when the post-buckling regime is determined via *linear* elasticity (dot-dash). Right: Plot of the difference \mathcal{D} in the prediction of $\delta\mathcal{V}$ via the alternative nonlinear models. $\mathcal{D} = \delta\mathcal{V}_{MR} - \delta\mathcal{V}_{NH}$ (solid), $\mathcal{D} = \delta\mathcal{V}_{HM} - \delta\mathcal{V}_{MR}$ (dotted), $\mathcal{D} = \delta\mathcal{V}_{HM} - \delta\mathcal{V}_{NH}$ (dashed) and $\mathcal{D} = \delta\mathcal{V}_{LIN} - \delta\mathcal{V}_{MR}$ (dot-dashed).

As can be seen from the left of Fig. 8, all curves are strongly nonlinear, exhibiting a softening behaviour under loading after the initial linear elastic behaviour pre-buckling at small pressures. As should be expected all four curves are initially identical with a slight modification in the post-buckling regime where the linear or nonlinear elastic model becomes important. However even in this regime the curve is fairly insensitive to the constitutive model employed, nonlinear models yielding almost identical results. The linear model is fairly close to the nonlinear predictions at these pressures but as pressure increases the linear results depart significantly as should be expected from this approximate theory.

In order to better compare the models, on the right of Fig. 8 we plot the *difference* between the relative volume change predicted by the different elastic post-buckling models. For example the difference between Horgan-Murphy and Mooney-Rivlin is calculated as $\mathcal{D} = \delta\mathcal{V}_{HM} - \delta\mathcal{V}_{MR}$ and analogously for the other two possibilities. Given the scale, it is clear that the difference between any of the nonlinear models is $O(10^{-4})$. We reiterate that at these pressures the linear elastic model is relatively close to the nonlinear models but at higher pressures there is a significant departure.

Although here we are predominantly interested in $p/\mu_m = O(1)$ we note with reference to Fig. 9, that for both *incompressible* nonlinear materials, as

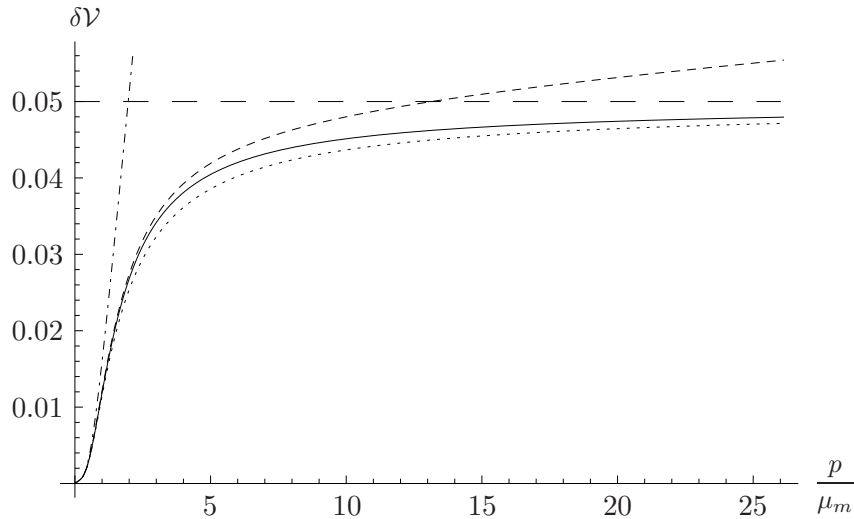


Figure 9: Prediction of $\delta\mathcal{V}$ for large values of p/μ_m with all parameters as given in Fig. 8 and plotted for Neo-Hookean (dotted), Mooney-Rivlin (solid) and slightly-compressible Horgan Murphy (dashed) nonlinear models as well as a linear elastic prediction (dot-dashed).

$p/\mu_m \rightarrow \infty$, $\delta\mathcal{V} \rightarrow 0.05$, as we should expect in that case (parameters chosen are those associated with Fig. 8). The Horgan-Murphy model (dashed) predicts a slightly different limit for $\delta\mathcal{V}$ as shown in Fig. 9 since this takes into account the slight compressibility of the matrix. The curve associated with the linear elastic model illustrates its unrealistic nature for large deformations.

5.2.2. Influence of volume fraction, shell properties and pressure law

We concluded in section 5.2.1 that the predicted curves are relatively insensitive to the nonlinear elastic model employed. As a result of this insensitivity, let us now model the matrix as an incompressible Mooney-Rivlin medium - a standard model for a rubber-like matrix medium. Thus, with the solid curve from Fig. 8 as a starting point, also plotted is a reference curve in Fig. 10, and let us vary other parameters in order to assess their influence. For each curve we keep all parameters fixed except one control parameter in order to assess its particular effect. Thus, the dashed curve in Fig. 10 corresponds to changing only the volume fraction of microspheres from $\Phi = 0.05$ to $\Phi = 0.1$. The dotted curve corresponds to incorporating Boyle's law (17) for the gas interior to the microsphere instead of constant pressure.

The thick dashed curve corresponds to softer shell material properties, i.e.

$$\mu_s = 0.126 \text{ GPa}, \quad \kappa_s = 0.21 \text{ GPa}, \quad (28)$$

and the dot-dashed curve is associated with slightly more compressible matrix material properties (for the linear elastic pre-buckling portion of the curve), i.e.

$$\mu_m = 1.2 \text{ MPa}, \quad \kappa_m = 0.4 \text{ GPa}. \quad (29)$$

These correspond to a Poisson's ratio of $\nu_m = 0.4985$.

Let us assess each one of these in turn. Increasing the microsphere volume fraction, whilst keeping their distribution fixed has the expected effect: the curve remains qualitatively similar, becoming relatively softer in the nonlinear regime. Incorporating Boyle's law should add some stiffness in the post-buckling regime and this can be seen in the figure; but its effect is rather modest. The dotted and solid curves are identical until the post-buckling effects become important, around $p/\mu_m = 0.2$, and then increased pressure interior to the microsphere does yield a small additional stiffness. Softer shell properties are expected to have a larger effect in the transition region from pre to post buckling as the shells will clearly buckle at lower pressures. This can clearly be seen in the figure; an order of magnitude change to the properties has modified the curve significantly. However, the insensitivity post-buckling can be seen by virtue of this curve and the solid curve remaining parallel in this regime. Finally, the small decrease in matrix Poisson's ratio corresponding to the dot-dashed curve yields the expected effect; the material becomes slightly softer in the linear region, recovering an identical nonlinear response to the reference Mooney-Rivlin case in the post-buckling region.

As perhaps should be expected, there is a great sensitivity to the material properties of the shell, but the model is relatively insensitive to other parameters.

5.2.3. Influence of probability distribution function parameters

Let us now take the Mooney-Rivlin reference curve (solid) as plotted in Fig. 8 and vary the distribution function parameters in F from those of the reference material $\hat{X}_0 = 0.01$ and $k = 8$. In Fig. 11 we plot the distribution function (left) and corresponding pressure-relative volume change curves (right) whilst keeping $k = 8$ fixed and varying \hat{X}_0 (top) and then keeping $\hat{X}_0 = 0.01$ fixed and varying k (bottom). As perhaps should be expected

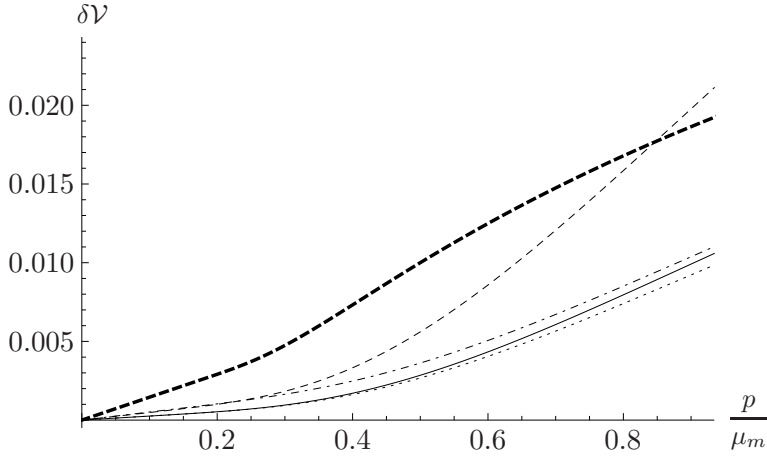


Figure 10: Parameter study for the predicted pressure-relative volume change curve. The solid curve corresponds to the parameters assumed in Fig. 8 with a Mooney-Rivlin matrix medium. We then vary one specific aspect of the model to assess sensitivity. Different curves correspond to: increasing microsphere volume fraction from $\Phi = 0.05$ to $\Phi = 0.1$ (dashed); incorporating Boyle’s law (17) for the gas interior to the microsphere instead of constant pressure (dotted); softer shell properties given by (28) (thick dashed); slightly more compressible matrix phase given by (29) (dot-dashed).

there is great sensitivity to the average shell thickness to radius ratio. This can be seen by the large modifications to the pressure-volume curves in the top-right figure. The main effect of varying k is the later (in terms of higher pressure) softening of the material, although its influence is less marked than variation in \hat{X}_0 . This information is useful from the viewpoint of knowing the correct type and distribution of microspheres to use in the composite.

Finally, we illustrate how the ‘kink’ in the load curve is associated primarily with the distribution function of the shell thicknesses. Let us choose $\hat{X}_0 = 0.01$ and successively increase k which has the effect of tending the distribution function towards a dirac delta function as can be seen in Fig. 12 where we take $k = 8$ (solid), $k = 50$ (dotted) and the limit as $k \rightarrow \infty$ (dashed). The limiting case when there is only one size of microsphere shell in the composite ($k \rightarrow \infty$) is reflected in the shape of the pressure-volume curve illustrated on the right of Fig. 12, manifested by a discontinuity in derivative of the curve. When k is made finite and reduced the curve becomes progressively smoother.

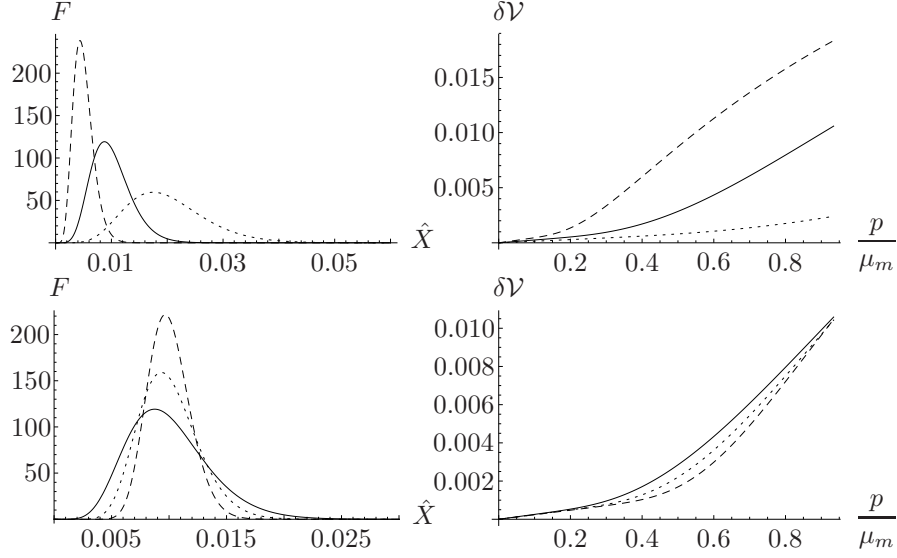


Figure 11: Plots of the distribution function (left) against shell thickness to radius ratio and corresponding pressure-relative volume change curves (right). The parameter $k = 8$ is held fixed and we vary \hat{X}_0 (top) whereas we keep $\hat{X}_0 = 0.01$ fixed and vary k (bottom). Specifically we take $\hat{X}_0 = 0.01, 0.02$ and 0.005 (solid, dotted and dashed respectively) (top) and $k = 8, 15$ and 30 (solid, dotted and dashed respectively) (bottom).

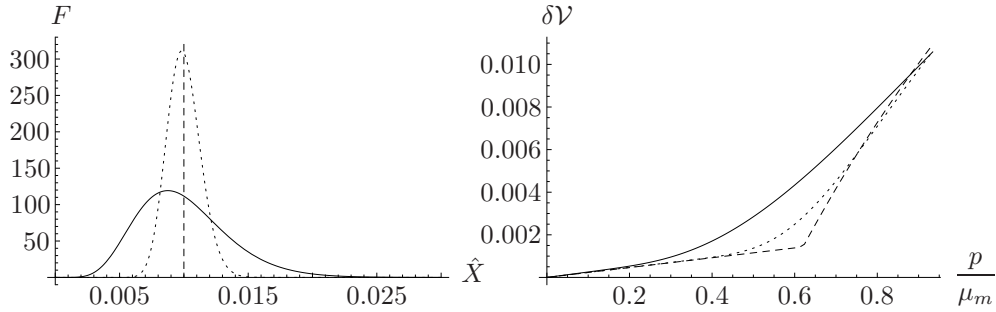


Figure 12: Illustrating how the shape of the load curve is modified in the limit $k \rightarrow \infty$. We choose $\hat{X}_0 = 0.01$ and take $k = 8$ (solid), $k = 50$ (dotted) and the limit as $k \rightarrow \infty$ (dashed). The limiting case when there is only one size of microsphere shell in the composite ($k \rightarrow \infty$) is reflected in the shape of the pressure-volume curve illustrated on the right, i.e. the appearance of a discontinuity in derivative of the curve. The curve becomes smoother in this region as k is progressively reduced.

6. Conclusions

We have presented a model that predicts the nonlinear *pressure-relative volume change* loading curve associated with a microsphere elastomeric composite material. The nonlinearity is induced by several mechanisms: (i) incorporating a distribution of sizes of spherical shells which thus buckle successively according to the applied load, (ii) modelling the post-buckling behaviour of the matrix as a nonlinear elastic material, (iii) incorporating Boyle’s law for the pressure interior to the microsphere in the post-buckling regime.

In this initial study we have neglected any interaction between microspheres both in terms of the buckling analysis and the determination of the change in volume of the composite. Therefore we anticipate that the model is valid only for low volume fractions of microspheres.

Parameter studies reveal that, although it appears important to include nonlinear behaviour in the post-buckling stage, the curves are largely insensitive to the chosen nonlinear elastic model. However the curves *are* particularly sensitive to the properties of the microsphere, including shell properties and the distribution of shell thickness, particularly the choice of mean shell thickness to radius ratio \hat{X}_0 . Furthermore, the shape of the ‘kink’ in the load curve is associated primarily with the distribution function of the shell thicknesses. The smaller k is, the smoother the transition to the nonlinear post-buckling state.

We have also seen that when Boyle’s law is incorporated in the post-buckling regime (the influence of a gas inside the shell pre-buckling is negligible as so is omitted in the model) there is competition between the softening of the material due to microsphere buckling and stiffening due to Boyle’s law. It transpired that the latter contribution is small, as is visible in the transition from pre to post buckling in Fig. 10. The near-incompressible nature of the matrix medium dictates that eventually the response of the composite will change, as the pressure increases, from an initial softening material to one which stiffens for large pressures ($p/\mu_m > O(1)$) as is seen in Fig. 9.

Note that in order to solve the post-buckling problem of a single spherical cavity embedded in a unbounded medium subject to inner and external hydrostatic pressure we used the theory of almost-incompressible materials, posing an asymptotic expansion for the Horgan-Murphy model (A.7) (see Horgan and Murphy (2009)).

Follow-on work will consider the accuracy of the buckling model, by com-

paring with alternative (e.g. Jones et al. (2008)) and new models. We shall also consider the effect of the interaction of microspheres on buckling. This is clearly important when volume fractions of microspheres become larger, a common case in practice.

Acknowledgements

The authors are grateful to the Engineering and Physical Sciences Research Council for funding this work via grant EP/H050779/1. They are also grateful to Dr Philip Cotterill and Dr Peter Brazier-Smith (Thales Underwater Systems Ltd) and Dr John Smith (DSTL) for their assistance regarding various aspects of this work. The authors are also grateful to Professor Bing Li (Technical Institute of Physics and Chemistry, Chinese Academy of Science) and Dr James Busfield (Queen Mary, University of London) for their willingness to provide figures 1 and 2 respectively, in order to reproduce them here.

Appendix A. Nonlinear elasticity theory

Appendix A.1. Incompressible theory

Given the deformation gradient \mathbf{F} , we compute the physical components of the left Cauchy-Green strain tensor $\mathbf{B} \equiv \mathbf{F}\mathbf{F}^T$ from (13) and find its first three principal invariants from

$$I_1 = \text{tr}\mathbf{B}, \quad I_2 = \frac{1}{2}[(\text{tr}\mathbf{B})^2 - \text{tr}\mathbf{B}^2], \quad I_3 = \det\mathbf{B}. \quad (\text{A.1})$$

For an isotropic incompressible hyperelastic solid, the Cauchy stress tensor \mathbf{T} is then related to the strain via

$$\mathbf{T} = -q\mathbf{I} + 2W_1\mathbf{B} - 2W_2\mathbf{B}^{-1}, \quad (\text{A.2})$$

where q is the Lagrange multiplier introduced by the incompressibility constraint, $W(I_1, I_2)$ is the strain-energy density and $W_i \equiv \partial W / \partial I_i$.

In the incompressible case, in order to model the nonlinear constitutive response of the matrix material, let us consider two alternative strain energy functions, the so-called neo-Hookean and Mooney-Rivlin models:

$$W_{\text{NH}} = \frac{\mu_m}{2}(I_1 - 3), \quad (\text{A.3})$$

$$W_{\text{MR}} = \frac{1}{2} \left(\frac{1}{2} + \gamma \right) \mu_m (I_1 - 3) + \frac{1}{2} \left(\frac{1}{2} - \gamma \right) \mu_m (I_2 - 3), \quad (\text{A.4})$$

where $\mu_m > 0$ is the shear modulus of the matrix (as introduced above) for infinitesimal deformations and γ is a non-dimensional constant in the range $-1/2 \leq \gamma \leq 1/2$.

Appendix A.2. Slightly-compressible theory

In the case of generally compressible materials, the Cauchy stress can be written as

$$\mathbf{T} = \beta_0 \mathbf{I} + \beta_1 \mathbf{B} + \beta_{-1} \mathbf{B}^{-1}, \quad (\text{A.5})$$

where

$$\begin{aligned} \beta_0(I_1, I_2, I_3) &= \frac{2}{\sqrt{I_3}} \left[I_2 \frac{\partial W}{\partial I_2} + I_3 \frac{\partial W}{\partial I_3} \right], \\ \beta_1(I_1, I_2, I_3) &= \frac{2}{\sqrt{I_3}} \frac{\partial W}{\partial I_1}, \\ \beta_{-1}(I_1, I_2, I_3) &= -2\sqrt{I_3} \frac{\partial W}{\partial I_2}. \end{aligned} \quad (\text{A.6})$$

A variety of strain energy functions can be proposed, but one in particular was described by Horgan and Murphy (2009) in the form

$$W_{\text{HM}} = \frac{\mu_m}{2} \left(\frac{1}{2} + \gamma \right) (I_1 - 3I_3^{1/3}) + \frac{\mu_m}{2} \left(\frac{1}{2} - \gamma \right) (I_2 - 3I_3^{2/3}) + \frac{\kappa_m}{2} (I_3^{1/2} - 1)^2 \quad (\text{A.7})$$

where γ is an arbitrary constant, μ_m is the infinitesimal shear modulus and κ_m is the infinitesimal bulk modulus. The latter two material parameters are usually related for an almost incompressible (slightly compressible) material through the additional assumption

$$\epsilon = \frac{\mu_m}{\kappa_m} \ll 1. \quad (\text{A.8})$$

Note from (A.7) that W_{HM} can be considered as a slightly compressible generalization of the incompressible Mooney-Rivlin strain energy function (A.4) since

$$W_{\text{HM}}(I_1, I_2, I_3 = 1) = W_{\text{MR}}(I_1, I_2). \quad (\text{A.9})$$

We proceed to solve the boundary value problem by posing the radial displacement as a regular asymptotic expansion in powers of ϵ , i.e.

$$r(R) = r_0(R) + \epsilon r_1(R) + \epsilon^2 r_2(R) + O(\epsilon^3), \quad (\text{A.10})$$

where

$$r_0(R) = (R^3 + \alpha)^{1/3} \quad (\text{A.11})$$

is determined from the incompressible theory (equivalently $\epsilon \rightarrow 0$). The correction terms $r_1(R)$ and $r_2(R)$ are the same order of magnitude as $r_0(R) - R$. Making use of the unconstrained theory our goal is to determine $r_1(R)$ and in order to do this it is necessary to retain terms of $O(\epsilon^2)$ in (A.10).

Let us expand the Cauchy stress tensor \mathbf{T} , whose form for the compressible problem is given in (A.5), in the form

$$\mathbf{T} = \mathbf{T}_0 + \epsilon \mathbf{T}_1 + O(\epsilon^2). \quad (\text{A.12})$$

Since β_0 in (A.6) involves the term $I_3 \partial W / \partial I_3$, the hydrostatic part of \mathbf{T}_0 involves the term r_1 (see Spencer (1970)) which is then determined in a manner described below. We write all other equations in the form of asymptotic expansions. In particular we note that

$$\text{div} \mathbf{T} = \text{div} \mathbf{T}_0 + \epsilon \text{div} \mathbf{T}_1 + O(\epsilon^2), \quad (\text{A.13})$$

and the traction boundary conditions must be written as

$$T_{rr}(R)|_{R \rightarrow \infty} = -p + 0\epsilon + O(\epsilon^2), \quad T_{rr}(A) = -p_{\text{IN}}^s - p_{\text{IN}}^b + 0\epsilon + O(\epsilon^2), \quad (\text{A.14})$$

noting that they give inhomogeneous conditions at leading order and homogeneous conditions at higher orders. Using these we can then equate terms at each order in ϵ and solve the resulting problems.

Using the boundary condition (A.14)₁ to leading order and the equilibrium equation $\text{div} \mathbf{T}_0 = 0$ we obtain the general expression for T_{0rr} ,

$$T_{0rr}(R) = -p - 2 \int_R^\infty \frac{dr_0(\rho)}{d\rho} \frac{T_{0rr}(\rho) - T_{0\theta\theta}(\rho)}{r_0(\rho)} d\rho. \quad (\text{A.15})$$

Imposing the leading order boundary condition (A.14)₂ then allows us to recover the relationship (20), i.e. the result associated with the incompressible solution (14).

Next equating (A.15) with the zeroth order term T_{0rr} found in (A.12), allows us to find a linear first order ordinary differential equation for r_1 , whose solution is given explicitly by

$$r_1(R) = \frac{2R^2 r_0^2 (-1 + 2\gamma) + R^4 (1 + 2\gamma) + R^3 r_0 \left(1 - 6\gamma - \frac{4p}{3\mu_m}\right) + 4C_1 r_0}{4r_0^3}, \quad (\text{A.16})$$

where C_1 is an integration constant to be determined. In order to determine C_1 we must continue our analysis to the next order i.e. we solve $\text{div}\mathbf{T}_1 = 0$. The first order balance equation is a linear second order differential equation for the unknown function $r_2(R)$ whose solution we do not reproduce here (for brevity, but also because we are primarily interested in $r_1(R)$). The function $r_2(R)$ involves two constants of integration which we shall call C_2 and C_3 . It is straightforward to determine that only one of these constants, say C_2 , is involved in the component T_{1rr} of the stress, in addition to C_1 . Using the $O(\epsilon)$ boundary conditions (A.14) for the stress \mathbf{T}_1 , it is then possible to determine both C_1 and C_2 . In particular since we are interested in only the first order correction to r_0 we state only C_1 which takes the form

$$C_1 = -\frac{\alpha_8\bar{a}^8 + \alpha_7\bar{a}^7 + \alpha_6\bar{a}^6 + \alpha_5\bar{a}^5 + \alpha_4\bar{a}^4 + \alpha_3\bar{a}^3 + \alpha_2\bar{a}^2 + \alpha_1\bar{a} + \alpha_0}{\left[480\bar{a}(A^3 + \bar{a}^3)(\bar{a}^2(1 - 2\gamma) + A^2(1 + 2\gamma))\mu_m\right]} \quad (\text{A.17})$$

where

$$\begin{aligned} \alpha_8 &= A(40p(7 + 6\gamma) - 3(83 + 4\gamma(43\gamma - 57))\mu_m), \\ \alpha_7 &= 240A^2(1 - 2\gamma)^2\mu_m, \\ \alpha_6 &= -20A^3(2\gamma - 1)(4p + 3(6\gamma - 1)\mu_m), \\ \alpha_5 &= 120A^4(4\gamma^2 - 1)\mu_m, \\ \alpha_4 &= -10A^5(p(4 + 8\gamma) + 3(5 + 4\gamma(9\gamma - 5))\mu_m), \\ \alpha_3 &= 16A^6(10p(2\gamma - 1) + 9\mu_m + 6\gamma(16\gamma - 9)\mu_m), \\ \alpha_2 &= 60A^7(4\gamma^2 - 1)\mu_m, \\ \alpha_1 &= -40A^8(1 + 2\gamma)(4p + 3(6\gamma - 1)\mu_m), \\ \alpha_0 &= 135A^9(1 + 2\gamma)^2\mu_m. \end{aligned}$$

In contrast to Faulkner (1971), here the constant C_1 depends on the boundary conditions via the presence of p and \bar{a} . Faulkner (1971) does *not* impose boundary conditions in the form (A.14) working instead with rather non-physical boundary conditions for the slightly compressible part of the deformation.

References

- Anson, L.W., Chivers, R.C., 1989. Ultrasonic propagation in suspensions – a comparison of a multiple scattering and an effective medium approach. J. Acoust. Soc. America 85, 535–540.

- Anson, L.W., Chivers, R.C., 1993. Ultrasonic velocity in suspensions of solids in solids – a comparison of theory and experiment. *J. Phys. D: Appl. Phys.* 26, 1566–1575.
- Ash, M., Ash, I., 2007. *Handbook of Fillers, Extenders, and Diluents*. Synapse Information Resources Inc.
- Baird, A.M., Kerr, F.H., Townend, D.J., 1999. Wave propagation in a viscoelastic medium containing fluid-filled microspheres. *J. Acoust. Soc. America* 105, 1527–1538.
- Bardella, L., Genna, F., 2001. On the elastic behavior of syntactic foams. *Int. J. Solids Structures* 38, 7235 – 7260.
- Ben Amar, M., Goriely, A., 2005. Growth and instability in elastic tissues. *J. Mech. Phys. Solids* 53, 2284 – 2319.
- Bose, S.K., Mal, A.K., 1974. Elastic waves in a fibre reinforced composite. *J. Mech. Phys. Solids* 22, 217–229.
- Brazier-Smith, P.R., 1999. A unified model for the properties of composite materials. Technical Report. Thales Underwater Systems Ltd.
- Brazier-Smith, P.R., 2010. Private communication. Discussion with Thales Underwater Systems Ltd.
- Carroll, M.M., 1988. Finite strain solutions in compressible isotropic elasticity. *J. Elasticity* 20, 65–92.
- Carroll, M.M., 1991a. Controllable deformations for special classes of compressible elastic solids. *Stability and Applied Analysis of Continuous Media* 1, 309–323.
- Carroll, M.M., 1991b. Controllable deformations in compressible finite elasticity. *Stability and Applied Analysis of Continuous Media* , 373–384.
- Chung, D.T., Horgan, C.O., Abeyaratne, R., 1986. The finite deformation of internally pressurized hollow cylinders and spheres for a class of compressible elastic materials. *Int. J. Solids Structures* 22, 1557 – 1570.
- Diaconu, I., Dorohoia, D., 2005. Properties of polyurethane thin films. *Journal of Optoelectronics and Advanced Materials* 7, 921 – 924.

- Ericksen, J.L., 1955. Deformations possible in every compressible, isotropic, perfectly elastic material. *J. Math. and Phys.* 34, 126–128.
- Faulkner, T.R., 1971. Finite dynamic deformations of an almost incompressible elastic spherical shell. *International Journal of Engineering Science* 9, 889 – 898.
- Fok, S.L., Allwright, D.J., 2001. Buckling of a spherical shell embedded in an elastic medium loaded by a far-field hydrostatic pressure. *The Journal of Strain Analysis for Engineering Design* 36, 535 – 544.
- Fu, Y., 1998. Some asymptotic results concerning the buckling of a spherical shell of arbitrary thickness. *International Journal of Non-Linear Mechanics* 33, 1111 – 1122.
- Gaunaurd, G., Uberall, H., 1982. Resonance theory of the effective properties of perforated solids. *J. Acoust. Soc. America* 71, 282–295.
- Gaunaurd, G.C., Callen, E., Barlow, J., 1984. Pressure effects on the dynamic effective properties of resonating perforated elastomers. *J. Acoust. Soc. America* 76, 173–177.
- Gent, A.N., Thomas, A.G., 1959. The deformation of foamed elastic materials. *J. Appl. Polymer Sci.* 1, 107–113.
- Gibson, L.J., Ashby, M.F., 1982. The mechanics of three-dimensional cellular materials. *Proc. Roy. Soc. A* 382, 43–59.
- Gupta, N., Woldesenbet, E., 2004. Microballoon wall thickness effects on properties of syntactic foams. *Journal of Cellular Plastics* 40, 461–480.
- Horgan, C.O., 1989. Some remarks on axisymmetric solutions in finite elastostatics for compressible materials. *Proc. Roy. Irish Acad. Sect. A* 89, 185–193.
- Horgan, C.O., 1995. On axisymmetric solutions for compressible nonlinearly elastic solids. *Z. Angew. Math. Phys.* 46, S107–S125. Theoretical, experimental, and numerical contributions to the mechanics of fluids and solids.
- Horgan, C.O., 2001. *Nonlinear Elasticity: Theory and Applications*. Cambridge University Press. chapter Equilibrium solutions for compressible

- nonlinear elasticity. Number 283 in London Mathematical Society Lecture Note Series, pp. 135–159.
- Horgan, C.O., Murphy, J.G., 2007a. Constitutive models for almost incompressible isotropic elastic rubber-like materials. *Journal of Elasticity* 87, 133–146. 10.1007/s10659-007-9100-x.
- Horgan, C.O., Murphy, J.G., 2007b. The effects of compressibility on inhomogeneous deformations for a class of almost incompressible isotropic nonlinearly elastic materials. *Journal of Elasticity* 88, 207–221.
- Horgan, C.O., Murphy, J.G., 2009. Compression tests and constitutive models for the slight compressibility of elastic rubber-like materials. *International Journal of Engineering Science* 47, 1232 – 1239.
- Jones, G.W., Chapman, S.J., Allwright, D.J., 2008. Axisymmetric buckling of a spherical shell embedded in an elastic medium under uniaxial stress at infinity. *The Quarterly Journal of Mechanics and Applied Mathematics* 61, 475–495.
- Kerr, F.H., Baird, A.M., 2002. Acoustic modelling of signature reduction materials for underwater applications, in: Abrahams, I., Martin, P., Simon, M. (Eds.), *IUTAM Symposium on Diffraction and scattering in fluids mechanics and elasticity*, Kluwer, Dordrecht. pp. 123–132.
- Koiter, W.T., 1969. The nonlinear buckling problem of a complete spherical shell under uniform external pressure. *Proceedings of the Koninklijke Nederlandse Akademie van Wetenschappen Royal Dutch Academy of Sciences Ser B* 72, 40–123.
- Kuster, G.T., Toksöz, M.N., 1974. Velocity and attenuation of seismic waves in two-phase media: Part I. Theoretical formulation. *Geophysics* 39, 587–606.
- Lakes, R., Rosakis, P., Ruina, A., 1993. Microbuckling instability in elastomeric cellular solids. *J. Mat. Sci.* 28, 4667–4672.
- Li, B., Yuan, J., An, Z., Zhang, J., 2011. Effect of microstructure and physical parameters of hollow glass microsphere on insulation performance 62, 1992 – 1994.

- Mackenzie, J.K., 1950. The elastic constants of a solid containing spherical holes. *Proc. Phys. Soc. Lond. B* 63, 2–11.
- Murphy, J.G., 1992. Some new closed-form solutions describing spherical inflation in compressible finite elasticity. *IMA J. Appl. Math.* 48, 305–316.
- Ogden, R.W., 1976. Volume changes associated with the deformation of rubber-like solids. *Journal of the Mechanics and Physics of Solids* 24, 323–338. Cited By (since 1996): 37.
- Ogden, R.W., 1978. Nearly isochoric elastic deformations: application to rubberlike solids. *J. Mech. Phys. Solids* 26, 37–57.
- Ogden, R.W., 1997. *Non-Linear Elastic Deformations*. Dover, New York. Reprint of Ellis Harwood Ltd, Chichester, (1984).
- Panigrahi, S.N., Jog, C.S., Munjal, M.L., 2008. Multi-focus design of underwater noise control linings based on finite element analysis. *Applied Acoustics* 69, 1141–1153.
- Parnell, W.J., Abrahams, I.D., Brazier-Smith, P.R., 2010. Effective properties of a composite half-space: Exploring the relationship between homogenization and multiple-scattering theories. *The Quarterly Journal of Mechanics and Applied Mathematics* 63, 145–175.
- Penn, R.W., 1970. Volume changes accompanying the extension of rubber. *Transactions of the Society of Rheology* 14, 509–517.
- Porfiri, M., Gupta, N., 2009. Effect of volume fraction and wall thickness on the elastic properties of hollow particle filled composites. *Composites Part B: Engineering* 40, 166 – 173.
- Shorter, R., Smith, J.D., Coveney, V.A., Busfield, J.J.C., 2010. Axial compression of hollow elastic spheres. *J. Mech. Materials Structures* 5, 693–705.
- Shorter, R., Thomas, A.G., Busfield, J.J.C., Smith, J.D., 2008. The physical behaviour of elastomers containing hollow spherical fillers, in: Boukamel, A., Lalarinandrasana, L., Meo, S., Verron, E. (Eds.), *Constitutive Models for Rubber V: Proceedings of the 5th European Conference*, Paris, France, 4-7 September 2007, Taylor and Francis, London. pp. 107–112.

- Spencer, A.J.M., 1970. The static theory of finite elasticity. *IMA Journal of Applied Mathematics* 6, 164–200.
- Tagliavia, G., Porfiri, M., Gupta, N., 2009. Vinyl ester-glass hollow particle composites: Dynamic mechanical properties at high inclusion volume fraction 43, 561–582.
- Truesdell, C., Noll, W., 1992. *The Nonlinear Field Theories of Mechanics*. Springer-Verlag, Berlin. second edition.
- Wang, A.S.D., Ertepinar, A., 1972. Stability and vibrations of elastic thick-walled cylindrical and spherical shells subjected to pressure. *International Journal of Non-Linear Mechanics* 7, 539 – 555.
- Waterman, P.C., Truell, R., 1961. Multiple scattering of waves. *J. Math. Phys.* 2, 512–537.
- Wesolowski, Z., 1967. Stability of an elastic, thick-walled spherical shell loaded by an external pressure. *Arch. Mech. Stosow.* 19, 3 – 23.